Novel Phosphotungstate-titania Nanocomposites from Aqueous Media

Jae-Hun Yang, Min-Kyung Kim, Ji-Hyun Son, Hyun-Jung Cho, and Young-Uk Kwon*

*Department of Chemistry, BK-21 School of Chemical Materials Science, and SKKU Advanced Institute of Nanotechnology, Sungkyunkwan University, Suwon 440-746, Korea. *E-mail: ywkwon@skku.edu*
Received March 16, 2007

We report a novel method to synthesize nanocomposites composed of titania nanoparticles and phosphotungstate ions with various composition ratios ranging from W/Ti = 12/10 to 12/500 by inducing the electrostatic interaction between the positively charged protonated titania sol-particles and the negatively charged phosphotungstate anions to flocculate and precipitate. The precipitates showed varied features depending on the composition. The precipitate from the tungsten-richest W/Ti = 12/10 reaction is amorphous in its powder X-ray diffraction (XRD), transmission electron microscopy (TEM), and Raman spectroscopy data. This material shows the Type II adsorption characteristics in its N_2-adsorption isotherm, but with quite low surface area of 34 m^2/g. To the contrary, the precipitates from the titanium-richer reactions (W/Ti = 12/50-12/500) are composed of anatase nanoparticles of 2-6 nm by XRD, TEM and Raman and show the Type I adsorption characteristics. The surface area linearly increases with the titanium content from 131 m^2/g for W/Ti = 12/50 to 228 m^2/g for 12/500. The precipitate from the reaction with the intermediate composition W/Ti = 12/20 is composed of anatase nanoparticles and does not have any pore accessible to N_2. With the wide variety of the physical properties of the precipitates, the present method can be a novel, viable means to tailor synthesis of nanocomposite materials. A formation mechanism of the precipitates is based on the electrostatic interactions between the titania nanoparticles and phosphotungstate ions.

Key Words : Electrostatic interaction, Intercluster salts, Nanocomposite, Phospotungstate, Titania nanoparticle

Introduction

Porous metal oxides have numerous applications including catalysis, separation, and adsorption due to their large surface areas and chemical activities.[1-4] This class of materials has the advantage of forming composites with various materials to tailor their functionalities. Notably, composites between polyoxometalate (POM) and titania have been studies widely in this regard.[5-10]

The general synthetic method of this class of materials is the sol-gel reactions starting from metal alkoxides in alcoholic solvents.[11-14] On the contrary, there have been quite few examples of producing porous metal oxides from aqueous systems probably because most of the metal ions of the oxides of interests are highly reactive in water so that their aqueous chemistry is practically uncontrollable.

According to the theories on colloids, sol particles in water can be kept from being aggregated by the repulsive electrostatic force between the particles. In order to increase the repulsive force between particles, sol solutions are typically prepared in strongly acidic conditions at which each particle is highly charged.[14,15] Counter ions adsorb on the surfaces of the sol particles to partially screen the surface potential. The degree of the screening depends on the nature of the counterions.[14,15] While the counter ions in most of the colloid literature are simple ions, we conjectured that larger anions such as POM ions could efficiently screen the surface potentials and induce precipitates, which could be a novel method to synthesize composites of metal oxides with POM ions. Also this may be a means to form gels in aqueous media. In fact, this idea arouse from our experience on 'intercluster salt' compounds. By combining cationic clusters such as $[Al_{13}(OH)_{39}]^{7+}$ and anionic clusters such as $[V_{10}O_{28}]^{6-}$, $[H_2W_{12}O_{40}]^{6-}$, and $[V_2W_4O_{19}]^{3-}$ in water, we were able to isolate solid materials in which the cationic and anionic clusters are alternately arranged as confirmed by their single crystal structures.[16-22] These intercluster salt compounds form because the solubility of a salt is minimized when the relative sizes of the interacting ions are close to each other.[23,24] The similar argument may apply to systems that have nanoparticles in the place of cluster ions. Although the particle size and shape of nanoparticles cannot be as uniform as those of POM ions, which fact precludes the possibility of forming well crystallized materials, there may be a strong driving force to form precipitate when there are nanoparticles of similar sizes and of opposite charges, which may be a novel synthetic method of nano-composites.

In the present paper, as a proof of the concept, we have chosen to study a system composed of 2-4 nm sized titania nanoparticles that have positive charges in acidic conditions and phosphotungstate ($PW_{12}O_{40}^{3-}$, PW) anions of about 1 nm. Under the right conditions including pH of the solution, the attractive interaction between titania nanoparticles mediated by PW ions becomes stronger than the repulsive force between themselves so that they form permanent precipitates. Herein, the details of the sample preparation and their characterization are reported.

Experimental

Synthesis. The composites were prepared by slowly increasing the pH of solutions containing $H_3PW_{12}O_{40}$ (Phosphotungstic acid, PWA) and titania nanoparticles to pH = 1. Composites were obtained from mixture solutions with the W/Ti molar ratios 12/10, 12/20, 12/50, 12/100, and 12/500. We will describe the detailed preparation of composite from the solution of W/Ti = 12/100; preparation of the other samples are similar except for the amounts of the reagents used. A titania sol solution was prepared by adding $TiCl_4$ (10 mL, 0.10 mol) dropwisely to a 6 M HCl aqueous solution (189 mL) with vigorous stirring while keeping the solution temperature below 1 °C with an ice-water bath followed by aging at 80 °C overnight. This method reportedly produces titania nanoparticles of 2-4 nm in size.[25] An aqueous PWA solution was prepared by dissolving 0.72 g (2.5×10^{-4} mol) of PWA into 30 mL of distilled water. The PWA solution was added to a 50 mL titania solution (0.025 mol). The pH-meter reading of this mixture solution was −0.65, and the solution was clear with no indication of the reaction between PW-species and titania sol particles. A 10 M NaOH solution was slowly added to the mixed solution with vigorous stirring until the pH became 1, during which the solution became turbid and formed a white precipitate. After aging overnight, the precipitate was isolated by centrifugation, washed five times with deionized water, and dried in an 80 °C oven.

Characterization. Powder X-ray diffraction (XRD) patterns of the samples were recorded on a Rigaku D/MAX-2200 Ultima diffractometer (2 kW) equipped with a Cu K_α (λ = 1.5415 Å) radiation in the 2θ range of 10-80°. Thermogravimetric analyses (TGA) were performed with a SDT 2960 thermogravimetric analyzer from room temperature up to 1000 °C with a heating rate of 5 °C/min under a N_2 atmosphere with a flow rate of 100 mL/min. Raman spectra were obtained with a Renishaw in Via Raman microscope using a 514 nm and 20 mW laser. Information on the particle morphology and size of the samples were acquired from high resolution transmission electron microscopic (HR-TEM) images by using JEOL JEM-3011 (300 kV). To obtain the elemental compositions, the samples were analyzed by an inductively coupled plasma atomic emission spectrometer (ICP-AES; Perkin-Elmer, OPTIMA 4300DV) and energy dispersive spectroscopy (EDS) with a FE-SEM equipped with a Link Oxford 7421 detector. The ICP-AES samples were prepared by the fusion-decomposition method, which involves forming a glassy material by heating with excess lithium metaborate, followed by dissolution in an acid solution.[26] Solid state ^{31}P MAS NMR measurements were performed with a 400 MHz solid state FT-NMR spectrometer (Bruker, DSX 400 MHz, B_o = 9.4 T), equipped with Bruker 4 mm probe. All powder samples were packed into 4-mm zirconia rotors sealed with Kel-F end caps. The ^{31}P NMR spectra were collected at the resonance frequency of 161.98 MHz with the magic angle spinning rate of 13 kHz and recycle delays of 20 s. N_2 adsorption-desorption isotherms of the samples were recorded by using Micromatrix TriStar 3000 at 77 K. All the samples were degassed at 403 K for 4 h under vacuum prior to the adsorption measurements. Particle size in solutions were measured with a Malvern Zetasizer $1000HS_A$ with 5 mW He-Ne laser (λ = 633 nm).

Results and Discussion

We have obtained PW-loaded titania composites of various compositions by reacting titania nanoparticles with PW-species in water. The reactions and the corresponding precipitates will be designated by their W/Ti ratios in the loaded solutions. Therefore, for example, 'W/Ti = 12/10' means both the solution of the atomic W/Ti ratio 12/10 and the precipitate from this solution. All of the reactions for W/Ti = 12/10, 12/20, 12/50, 12/100, and 12/500 produced similar-looking white precipitates. We also prepared PW-free (titania only) sample by the same procedure for the reference purpose.

The titania nano-sol solution was prepared under a strongly acidic condition with the pH-meter reading of −1.4. Addition of a PWA solution raised the pH to −0.55 (W/Ti = 12/10) ~ −0.98 (12/500) depending on the amount of the PWA solution. The solutions were transparent indicating no interaction between the titania nano-sol particles and PW species. In order to induce the precipitates, we added a 10 M NaOH solution dropwisely. In case of the PW-free solution, upon adding each drop of NaOH solution, the solution formed instantaneous flocculates which re-dissolved upon stirring. However, for the solutions containing PWA, there remained small amounts of flocculates that made the solutions turbid although most of the flocculates re-dissolved into the solution. The time required for the re-dissolution increased with the increase of pH. As the pH increased to 1, there formed a large amount of permanent flocculates in the solutions. Therefore, we have chosen the condition of pH 1 for the precipitate formation. Upon storing overnight after adjusting the pH at 1, there formed white precipitates regardless the loaded composition. These were isolated by centrifugation and washed with distilled water. After drying at 80 °C overnight, the precipitates turned into pale ivory-colored hard gels.

Figure 1 shows the compositions of the precipitates obtained from ICP-AES and EDS data. These data sets agree reasonably well with each other. The EDS spectra showed that the precipitates were mainly composed of Ti, W, and O; there was no peak for Na in any of the composite samples and the two Ti-richest samples showed trace amounts of Cl (0.79 at% in 12/100 and 1.34 at% in 12/500); the PW-free titania showed higher Cl content of 2.41 at% and Na of 0.37 at%. The compositions of the precipitates reflect those of the loaded compositions of starting solutions. However, the W-content in the precipitate tend to be smaller than that of the starting solution especially for the W-richer cases such as W/Ti = 12/20 and 12/10 probably because of the high solubility of PWA.

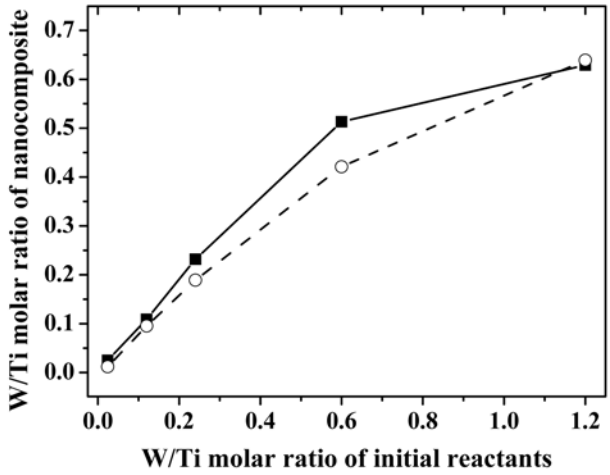

Figure 1. Variation of the composition of the titania-PW composites depending on the W/Ti molar ratio of reacting solutions determined by EDS (rectangular, solid line) and ICP-AES (circle, broken line).

According to the TGA analyses, all the samples showed single step weight losses by 12-17% which were completed at below 400 °C (not shown). These weight losses could be assigned to the desorption of the entrapped and coordinated water molecules and dehydroxylation.

The total mass of the dried precipitate gradually increased with the increase of the W-content from 1.2 g (W/Ti = 12/500) to 3.5 g (W/Ti = 12/10) per 0.025 mole of $TiCl_4$ used. However, by taking the TGA and elemental analysis data into consideration, the yields are more or less constant throughout the series with 46 ± 2% based on Ti, but increase with the decrease of the W-content from 26% for W/Ti = 12/10 to almost 100 % for 12/500 based on W.

The XRD patterns in Figure 2 show clear distinction between W/Ti = 12/10 precipitate and the others. The W/Ti = 12/10 pattern shows only a very broad peak at 2θ = 28° indicating an amorphous phase while the patterns of the others can be identified as that of anatase phase with peaks at 25.3° (101), 37.8° (004), 48.1° (200), 54.0° (105), 62.8° (204), and 68.8° (116) (the number in the bracket are diffraction indices based on the anatase structure, JCPDS-832243). The broad peaks suggest that these materials are composed of very small crystalline domains. By using the Scherrer equation for the (101) peaks,[27] the crystallite sizes were determined to be about 2-6 nm, suggesting that the initial titania particles did not grow in size during the sample preparation. The XRD pattern of W/Ti = 12/20 sample shows that it is a mixture between anatase and the amorphous material as seen in W/Ti = 12/10. The TEM images (Figure 3) also show that the precipitates other than W/Ti = 12/10 are composed of titania nanoparticles of a few nm in size. The number density of the titania nanoparticles increases with the Ti-content. It is noteworthy that the W/Ti = 12/10 sample does not show any indication for crystalline phase in its TEM image, in good agreement with the XRD data.

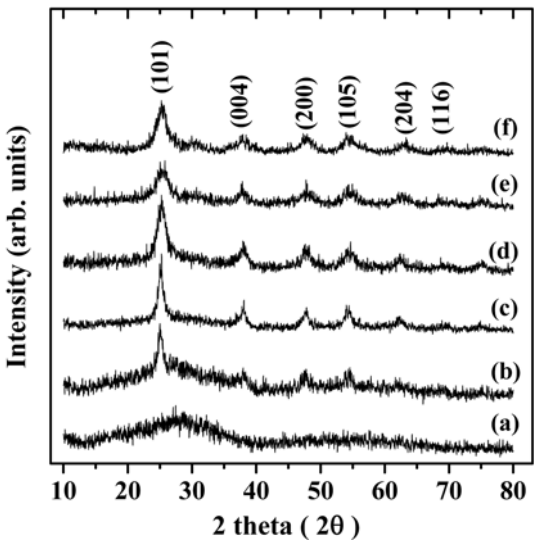

Figure 2. Powder X-ray diffraction patterns of the titania-PW composites; (a) W/Ti = 12/10, (b) 12/20, (c) 12/50, (d) 12/100, (e) 12/500, and (f) PW-free titania (The indices are for the anatase phase).

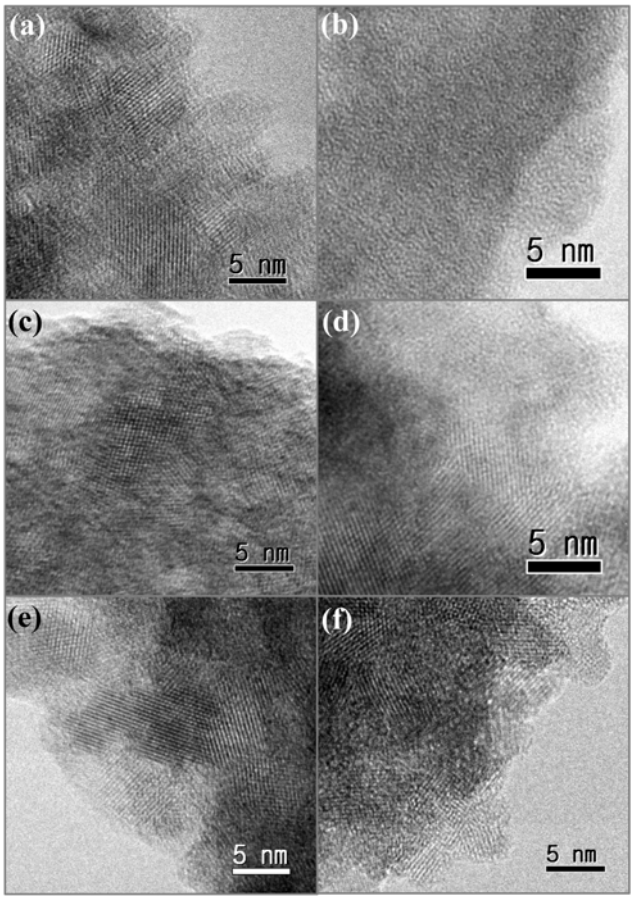

Figure 3. Transmission electron microscopic images of the titania-PW composites; (a) PW-free TiO_2, (b) W/Ti = 12/10, (c) 12/20, (d) 12/50, (e) 12/100 and (f) 12/500.

The presence of anatase nanaoparticle in the precipitates with high Ti-contents and the absence of it in the W/Ti = 12/10 sample were further confirmed by Raman spectroscopy.

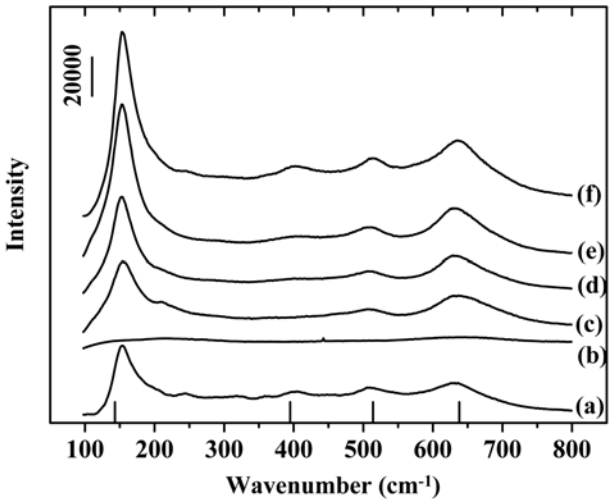

Figure 4. Raman spectra of the titania-PW composites; (a) PW-free TiO_2, (b) W/Ti = 12/10, (c) 12/20, (d) 12/50, (e) 12/100 and (f) 12/500. The bars at the bottom are the peak positions for highly crystalline anatase.

(Figure 4) Raman spectroscopy is well-known for its ability to distinguish the three titania phases and the degree of crystallinity. Single crystalline anatase was reported to show Raman peaks at 143 (E_g), 195 (E_g), 395 (B_{1g}), 514 (A_{1g} and B_{1g}), 638 (E_g) cm^{-1}.[28-35] The spectra of the precipitates other than W/Ti = 12/10 all show these peaks, except the weak one at 195 cm^{-1}, with their positions shifted. The peak positions of our samples are 153-156 (E_g), 401-403 (B_{1g}), 510-512 (A_{1g} and B_{1g}), and 630-633 (E_g) cm^{-1} (in increasing order of energy, the second E_g peak at 195 cm^{-1} was too weak to be observed), and these peak shifts indicate poorly crystalline anatase. On the contrary, the W/Ti = 12/10 sample shows no peaks that can be assigned to anatase. The Raman data are in good agreement with the XRD and TEM results.

Above observations and analysis data all indicate that the PW ions play an important role in the structure of composites as well as the formation process. Based on our observations and the principles of chemical interactions, we propose the formation process of precipitate as in the following:

The starting titania sol solution could be stable because of the repulsive forces caused by the highly positive surface charge in the strong acidic condition (pH = ~ −1.5). The addition of a base into this solution (when there is no PWA added) gives two major effects. One is the reduction of the titania surface charge by neutralization and the other is the increase of the electrolyte concentration. Both effects can reduce the repulsive forces between the titania nanoparticles and form flocculates and, then, precipitates, explaining the formation of a precipitate from the PW-free titania solution. There might be hydrolysis reactions between the titania nanoparticles occurring, but to a very small extent because of the strongly acidic condition of pH ≤ 1. The presence of PW-species in the solution could induce an additional type of interaction. The addition of a PWA solution to the titania solution raised the pH to −0.5 ~ −1.0, but such a change did not make any difference in terms of inter-particle interactions. Titania sol-particles would remain still highly charged, and a large fraction of PWA would remain protonated; there could be no interaction between these species. As pH was further increased, the strongly acidic PWA became PW-ions ($H_{3-x}PW_{12}O_{40}^{x-}$, x ~ 3 > 0) and could start to exert electrostatic interactions with the positively charged titania sol-particles to form aggregates. With the multiple negative charge and high polarizability,[8] PW-ions can screen the surface charges of the titania nanoparticles efficiently, causing aggregation of titania sol-particles with the PW-ions located between them. Alternatively, the formation of precipitate can be viewed as the result of the attractive interaction between the two oppositely charged species, PW-ions and titania sol-particles. The argument used to explain the formation of intercluster salts seems to apply to these cases. That is, the closer the sizes of anion and cation, the stronger becomes the lattice energy over hydration energy of the ions, and the stronger the tendency to form precipitates.

Table 1. Average particle sizes of re-dispersed titania-PW composites measured by a Zetasize analyzer

	Particle size (nm)	Polydispersity[a]
PW-free TiO_2	93	0.65
12/10	444	0.25
12/20	367	0.12
12/50	423	0.20
12/100	382	0.42
12/500	371	0.25

[a]The width of the distribution.

The particle size was measured on the suspension prepared by re-dispersing the precipitates into distilled water (Table 1) using a Zetasize analyzer. The particle sizes of the PW-containing titania composites (370-440 nm) are much larger than the PW-free titania (93 nm). It is remarkable that even a small amount of PW-ions can induce such a dramatic change of particle size (*i.e.*, compare 371 nm of W/Ti = 12/500 and 93 nm of PW-free titania) but the concentration of PW-ions does not matter as long as there are PW-ions in the solution (*i.e.*, compare 371 nm of W/Ti = 12/500 and 444 nm of W/Ti = 12/10). These observations can be explained by considering that the electrostatic interaction between PW-ions and titania sol-particles is a strong, long range interaction; the PW-ions and titania sol-particles form instantaneous aggregates that function as the nuclei on which further aggregation of titania takes place. Without the PW-ions, the nucleation process is retarded to result in smaller aggregates. In Figure 5, we show a schematic drawing of the structures of the precipitates with different compositions.

Above proposed mechanism also can explain the other experimental data. When the solution composition was such that the total charge of PW-ions exceeded that of the titania nanoparticles, which appeared to be the case for W/Ti = 12/10 solution, most of the titania sol-particles were surrounded by PW-ions and isolated from one another in the precipitate. The isolation of individual titania particles prohibited any

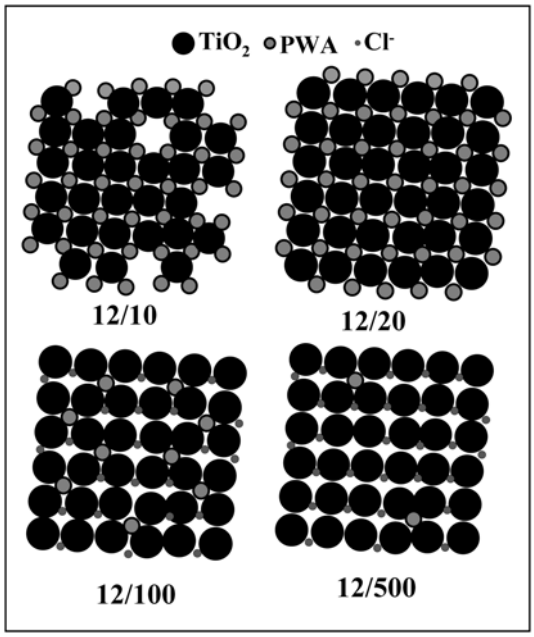

Figure 5. Schematic representation of the structures of the titania-PW composites with various W/Ti ratios.

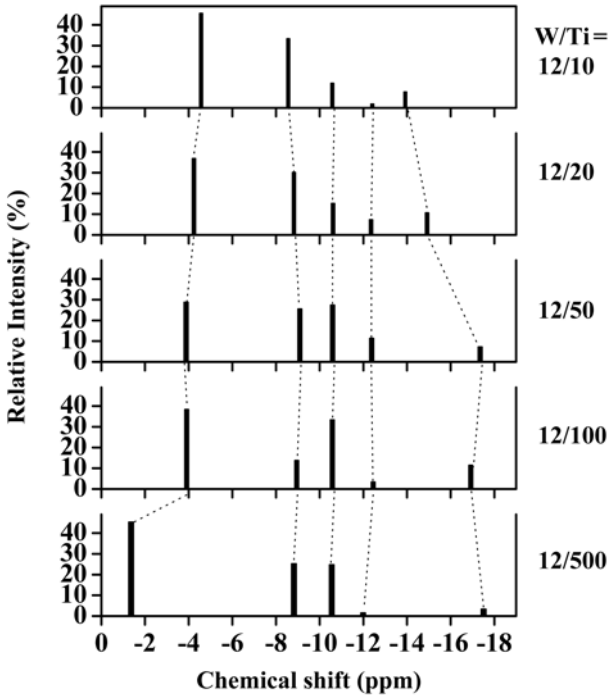

Figure 6. Variations of the peak positions and intensities for ^{31}P MAS NMR spectra of PW-titania nanocomposites with the W/Ti ratios.

secondary growth of the titania species, explaining the absence of any crystalline titania phase in its XRD, TEM and Raman data. To the contrary, as soon as there were excess titania species such as the other compositions (W/Ti = 12/20 - 12/500), the precipitates had regions where titania sol-particles were in close contact with one another, allowing development of crystalline anatase. If there were no or very few PW-ions present, some Cl^- ions could be incorporated between the titania particles in order to compensate the surface charge of excess titania.

The precipitates were also studied with ^{31}P solid state NMR spectroscopy to probe the states of the PW ions. From a ^{31}P NMR study on a PWA-impregnated titania particles, Edwards *et al.* reported five distinctive chemical shifts at −4 ppm (with a relative intensity 3%), −8 ppm (3%), −11 ppm (38%), −13 ppm (16%), −16 ppm (40%) for P.[36] According to their peak assignment, the peak at around −4 ppm is due to the phosphate species released from the fragmentation of PWA, the peak at −8 ppm to the W_nO_y-O_3P-OH of the '11-defect PWA' resulting from the loss of one W from PWA, the peak at −11 ppm to $(Ti\text{-}OH^+_2)_2(HPW_{12}O_{40}^{2-})$, the peak at −13 ppm to $(Ti\text{-}OH^+_2)(H_2PW_{12}O_{40}^-)$, and the peak at −16 ppm to PWA adsorbed on the surface. 94% of the PW-species in their sample remained unbroken. The variations of the peak positions and relative intensities with the W/Ti ratio of our samples are plotted in Figure 6. Compared with the literature data, the PW-species in our system appears to have undergone more severe fragmentation, with the two peaks at lower fields much stronger. This seems reasonable in view that PWA in our system is more extensively surrounded by titania nanoparticles, and the titania surfaces in our system are more highly charged, exerting stronger electric fields around PW-ions. Additionally, the heat treatment at 80 °C to dry the samples probably facilitated the fragmentation process further.

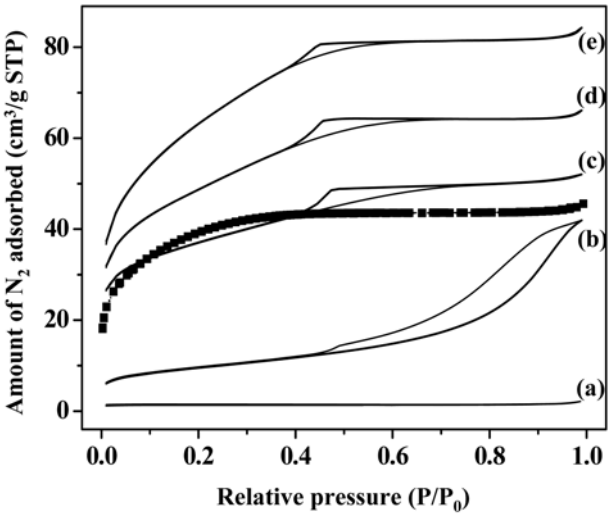

Figure 7. N_2 adsorption-desorption isotherms of the titania-PW composites; (a) W/Ti = 12/20, (b) 12/10, (c) 12/50, (d) 12/100, and (e) 12/500. ■ indicates PW-free TiO_2.

The N_2 adsorption-desorption isotherms for the composites are shown in Figure 7. Except nanocomposites with high PWA contents such as W/Ti = 12/10, the adsorption isotherms of all the nanocomposites (W/Ti = 12/20, 12/50, 12/100, 12/500) and PW-free titania could be classified as the Type I according to the BDDT (Brunauer, Deming, Deming, and Teller) classification,[37-39] characteristic for microporous materials. Although W/Ti = 12/20 has a poor

Table 2. Porous properties of titania-PW composites

Reacting molar ratio (W/Ti)	Specific Surface Area (m^2/g)		Pore volume (cm^3/g)	
	S_{BET}	S_{micro}[a]	V_{total}	V_{micro}[b]
12/10	34	7	0.065	0.003
12/20	4.3	–	0.003	–
12/50	131	112	0.081	0.059
12/100	172	168	0.10	0.091
12/500	228	223	0.13	0.12
PW-free TiO_2	144	142	0.071	0.067

[a,b]calculated by t-plot method

adsorption property, it also shows a Type I adsorption curve. These isotherms of Ti-rich samples indicate that aggregation between the titania sol-particles lead to the formation of micropores. Therefore, it appears that, even though the aggregation between the titania sol-particles is the major cause for the Type I adsorption behaviors of the Ti-rich composites, the PW ions play an important role in determining the pore structure. This point is especially clear when the isotherms of the W/Ti = 12/500 (with only 2.4 at% of W) and the PW-free titania are compared.

The adsorption isotherm of W/Ti = 12/10 is quite different from those of W/Ti = 12/50 - 12/500 and PW-free titania. This material shows the Type II curve, which is the characteristic of non-porous materials. The different adsorption behavior of W/Ti = 12/10 from the other composites can be attributed to the different structures, namely, the former is composed of alternating PW-ions and titania particles while the others are composed of aggregated titania mainly.

The porous properties calculated from the N_2 adsorption-desorption isotherms are summarized in Table 2. The BET specific surface areas are in the range of 4.3 - 228 m^2/g and the total pore volumes are in the range of 0.003 - 0.12 mL/g. As can be seen in Table 2, the specific surface area and the pore volume are the smallest (4.3 m^2/g, 0.003 mL/g) at W/Ti = 12/20, and these values linearly increase with the Ti mole fraction to the total metal content in the composite. Probably, the packing of titania and PW ions in W/Ti = 12/10 is efficient and leaves only a small fraction of surface that can adsorb N_2. The total absence of N_2 adsorption of W/Ti = 12/20 is rather surprising, in which there are no pores of N_2 molecule to access. These N_2 adsorption-desorption data are in good agreement with the schematic structural models suggested in Figure 5. Presently, we do not have any good explanation for this observation. It seems that this is caused by the efficient packing between the titania nanoparticles and PW-ions.

In order to understand the microporosity of the composites, we analyzed the adsorption isotherm data by the t-plot method as shown in Figure 8.[37-41] The Ti-rich composites (W/Ti = 12/50-12/500) and PW-free titania show the characteristic curves of micorporous materials, that is, the curves deviate from the linearity in the higher t-values, with reduced slopes in this region. However, the curve for W/Ti = 12/10 remains linear even up to high t-value region, indicating the property of non-porous solids. From the t-plots, we could calculate the micorpore volumes and the micropore surface areas as summarized in Table 2. Except for W/Ti = 12/10, the micropore volumes and the micropore surface areas of the composites are more than 80% of the total pore volumes and the BET surface areas, suggesting that these composites can be considered as microporous materials.

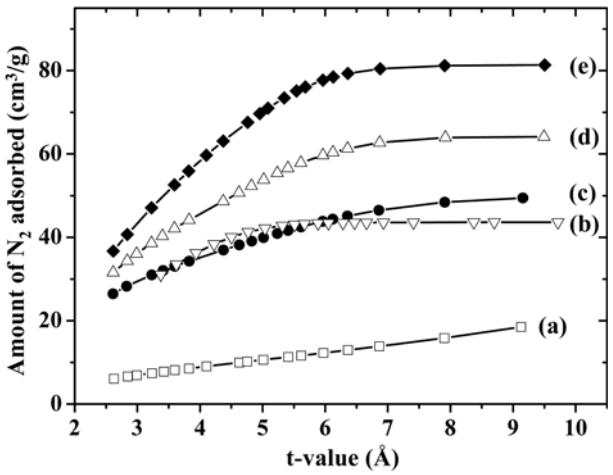

Figure 8. t-plots constructed from the N_2 adsorption data of titania-PW composites; (a) W/Ti = 12/10, (b) PW-free TiO_2, (c) 12/50, (d) 12/100, and 12/500.

Conclusions

In this study, we looked into previously neglected or avoided aspects of aqueous colloid systems composed of sol particles with a few nm in size. Instead of avoiding precipitate formation, we have intentionally included PW-ions into titania sol-particle solutions to induce precipitates. By controlling the pH, we could induce electrostatic interactions between the positively charged titania nanoparticles and the negatively charged PW ions. Under such a condition, we found that the PW ions could function as the mediating ions between the titania sol-particles to hold them to form precipitates. Depending on the starting composition of the solution, other types of reactions occur to influence the nature of the precipitates such as the crystallinity and porosity, which may prove to be an efficient way to tailoring materials. We believe that our results demonstrate the possibility of the aqueous process to form porous materials. To the best of our knowledge, there is no literature example of forming titania composite from aqueous medium besides impregnating POMs into titania powders.

Furthermore, this study revealed novel materials with unusual features such as the ‘pore-less’ W/Ti = 12/20 and the ‘structure-less’ W/Ti = 12/10. Further studies to understand the details of their microscopic and mesoscopic structural features and their potentials for applications are under current investigation in our group.

Acknowledgements. This work was supported by the Korea Research Foundation Grant funded by the Korean

Government (MOEHRD) (KRF-2005-005-J11903 and KRF-2006-311-C00369). This work is also supported by the Center for Nanotubes and Nanocomposites at SKKU.

References

1. Shchukin, D. G.; Caruso, R. A. *Chem. Mater.* **2004**, *16*, 2287.
2. (a) Barton, T. J.; Bull, L. M.; Klemperer, W. G.; Loy, D. A.; McEnaney, B.; Misono, M.; Monson, P. A.; Pez, G.; Scherer, G. W.; Vartuli, J. C.; Yaghi, O. M. *Chem. Mater.* **1999**, *11*, 2633. (b) Jhung, S. H.; Yoon, J. W.; Kim, H. K.; Chang, J. S. *Bull. Korean Chem. Soc.* **2005**, *26*, 1075.
3. Carreon, M. A.; Guliants, V. V. *Eur. J. Inorg. Chem.* **2005**, *1*, 27.
4. Shimizu, Y.; Hyodo, T.; Egashira, M. *Catal. Surv. Asia* **2004**, *8*, 127.
5. Li, L.; Wu, Q. Y.; Guo, Y. H.; Hu, C. W. *Micropor. Mesopor. Mater.* **2005**, *87*, 1.
6. Hayashi, K.; Takahashi, M.; Nomiya, K. *Dalton Transactions* **2005**, *23*, 3751.
7. Hayashi, K.; Murakami, H.; Nomiya, K. *Inorg. Chem.* **2006**, *45*, 8078.
8. He, T.; Yao, J. N. *Progress in Materials Science* **2006**, *51*, 810.
9. Bai, B.; Zhao, J. L.; Feng, X. *Mater. Lett.* **2003**, *57*, 3914.
10. Yang, Y.; Guo, Y. H.; Hu, C. W.; Jiang, C. J.; Wang, E. B. *J. Mater. Chem.* **2003**, *13*, 1686.
11. Zhu, J.; Chen, F.; Zhang, J.; Chen, H.; Anpo, M. *J. Photochem. Photobiol. A* **2006**, *180*, 196.
12. Su, C.; Tseng, C. M.; Chen, L. F.; You, B. H.; Hsu, B. C.; Chen, S. S. *Thin Solid Films* **2006**, *498*, 259.
13. Pakhomov, N. A.; Buyanov, R. A. *Kinet. Catal.* **2005**, *46*, 669.
14. Brinker, C. J.; Scherer, G. W. *Sol-Gel Science*; Academic Press: Boston, 1990; Chap. 2, p 4.
15. Myers, D. *Surfaces, Interfaces, and Colloids*; VCH Publishers: New York, 1991; Chap. 10.
16. Son, J. H.; Kwon, Y. U. *Inorg. Chim. Acta* **2005**, *358*, 310.
17. Son, J. H.; Kwon, Y. U. *Inorg. Chem.* **2004**, *43*, 1929.
18. Son, J. H.; Kwon, Y. U.; Han, O. H. *Inorg. Chem.* **2003**, *42*, 4153.
19. Son, J. H.; Choi, H.; Kwon, Y. U.; Han, O. H. *J. Non-Crystal Solid* **2003**, *318*, 186.
20. Son, J. H.; Kwon, Y. U. *Bull. Kor. Chem. Soc.* **2001**, *22*, 1224.
21. Son, J. H.; Choi, H.; Kwon, Y. U. *J. Am. Chem. Soc.* **2000**, *122*, 10492.
22. Choi, H.; Kwon, Y. U.; Han, O. H. *Chem. Mater.* **1999**, *11*, 1641.
23. Morris, D. F. C. *Structure Bonding* **1969**, *6*, 157.
24. Huheey, J. E. *Inorganic Chemistry*, 3rd ed.; Harper & Row: New York, 1983; Chap. 6.
25. Liu, Y.; Claus, R. O. *J. Am. Chem. Soc.* **1997**, *119*, 5273.
26. Bain, D. C.; Smith, B. F. L. In *A Handbook of Determinative Methods in Clay Mineralogy*; Wilson, M. J., Ed.; Chapman and Hall: New York, 1987; p 253.
27. Cullity, B. D. *Elements of X-ray Diffraction*, 2nd ed.; Addison-Wesley Publishing Company: California, 1978; p 101.
28. Wang, C.; Deng, Z. X.; Li, Y. *Inorg. Chem.* **2001**, *40*, 5210.
29. Zhang, J.; Li, M.; Feng, Z.; Chen, J.; Li, C. *J. Phys. Chem. B* **2006**, *110*, 927.
30. Wang, C.; Geng, A.; Guoa, Y.; Jiang, S.; Qu, X.; Li, L. *J. Colloid Interf. Sci.* **2006**, *301*, 236.
31. Zhang, W. F.; He, Y. L.; Zhang, M. S.; Yin, Z.; Chen, Q. *J. Phys. D: Appl. Phys.* **2000**, *33*, 12.
32. Choi, H. C.; Jung, Y. M.; Kim, S. B. *Bull. Kor. Chem. Soc.* **2004**, *25*, 426.
33. Bersani, D.; Lottici, P. P.; Ding, X. Z. *Appl. Phys. Lett.* **1998**, *72*, 73.
34. Lagarec, K.; Desgreniers, S. *Solid State Commun.* **1995**, *94*, 519.
35. Zhao, Y.; Lee, U. H.; Suh, M.; Kwon, Y. U. *Bull. Kor. Chem. Soc.* **2004**, *25*, 1341.
36. Edwards, J. C.; Thiel, C. Y.; Benac, B.; Knifton, J. F. *Catal. Lett.* **1998**, *51*, 77.
37. Gregg, S. J.; Sing, K. S. W. *Adsorption, Surface Area and Porosity*; Academic Press: New York, 1982.
38. Rouquerol, F.; Rouquerol, J.; Sing, K. *Adsorption by Powders and Porous Solids; Principles, Methodology and Applications*; Academic Press: London, 1999.
39. Han, Y. S.; Yamanaka, S.; Choy, J. H. *Appl. Catal. A* **1998**, *174*, 83.
40. Park, J. H.; Yang, J. H.; Yoon, J. B.; Hwang, S. J.; Choy, J. H. *J. Phys. Chem. B* **2006**, *110*, 1592.
41. Han, Y. S.; Yamanaka, S.; Choy, J. H. *J. Solid State Chem.* **1999**, *144*, 45.